REVIEW OF RESEARCH
IMPACT FACTOR : 5.7631(UIF) UGC APPROVED JOURNAL NO. 48514 ISSN: 2249-894X
VOLUME - 8 | ISSUE - 5 | FEBRUARY - 2019

# SYNTHESIS, STRUCTURAL AND OPTICAL PROPERTIES OF ALUMINIUM DOPED ZnO NANOPARTICLES

**Swati R. Gawali**
**Department of Physics, CES's Dr. A. B. Telang Sr. College, Nigdi, Pune .**

**ABSTRACT :**

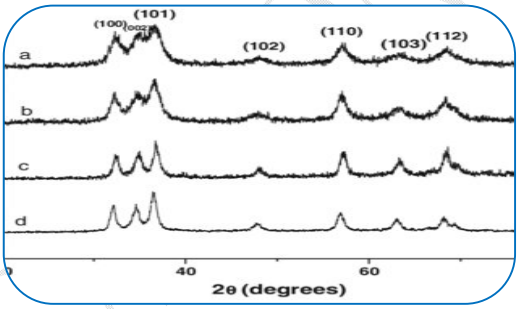


*In recent years plasmonics and metamaterials have attracted research community due to their wide applications in sub-diffraction imaging [1], invisibility cloaks [2], material with negative refractive index [3] and so on. In these applications noble metal materials are used as the conventional and primary building blocks of plasmonic optical metamaterials [4]. As compared with noble metals, semiconductors like ZnO, $TiO_2$ with appropriately doped material exhibits better results in the area of plasmonics and metamaterial applications [5, 6]. ZnO is an n-type semiconductor material with the properties like low cost, abundant availability in nature, non-toxicity, pollution free, suitability of doping, thermally stable and Due to these properties this material is widely studied in various applications like ultraviolet light emitters, solar cells, piezoelectric transducers, electromagnetic interference (EMI) shielding, radio frequency interference (RFI) shielding and so on [7-12].*

**KEYWORDS :** *attracted research community , radio frequency interference (RFI) , electromagnetic interference (EMI).*

## 1. INTRODUCTION:

ZnO also possesses a wide band-gap of 3.3 eV in the near UV region [13] and a large excitation binding energy of the order of 60 meV [14]. This characteristic makes this material transparent in the visible range. Hence it possesses low efficiency (5%) in the sunlight. To enhance the solar efficiency it is important to decrease the wide band gap and thereby increase the absorption of the solar radiations. This can be achieved by tailoring the electronic structure of the ZnO nanoparticles. Doping is the simplest and most effective way for this purpose. Group III materials such as Aluminium, Manganese, Indium, Fluorine and Gallium can be the suitable candidates for doping in the ZnO nanoparticles and are used to alter the catalytic, electrical and optical properties [15 – 17] of the ZnO nanoparticles. Among all these aluminium is a preferable dopant due to its properties such as good conductivity, good transparency in the visible region as well as low resistivity [18] and can be a better candidate for preparing a transparent conductive composite. AZO nanoparticles have been synthesized by various methods of synthesis like coprecipitation method [19], solvothermal method [20], pulsed laser deposition method [21], thermal evaporation method [22], magnetron sputtering method [23] and vapor deposition method [24]. Apart from producing monosized nanoparticles the sol-gel method is simple, easily reproducible and economically cheap and hence this method has attracted many researchers to synthesize the AZO nanoparticles.

In the present work we demonstrate the synthesis of undoped and aluminium doped ZnO nanoparticles by the sol-gel method. The effect of aluminium doping on the structural and optical properties of undoped ZnO nanoparticles is investigated and presented in the current paper.

## 2. EXPERIMENTAL DETAILS:

Undoped and aluminium doped zinc oxide nanoparticles were synthesized by the sol-gel route. A series of Al doped ZnO nanoparticles was prepared by incorporating the molar percentages of aluminium as 0.0%, .5% and 1.0% into the ZnO nanoparticles. Aluminium nitrate [$Al(NO_3)_3.9H_2O$], zinc acetate [$Zn(CH_3COO).2H_2O$] and citric acid ($C_6H_8O_7$) were used as the precursors. All the chemicals were of analytical grade obtained from Merck Company Ltd. and used as such. Distilled water is used as a solvent. Initially aqueous solutions of aluminium nitrate and zinc acetate were prepared separately under constant stirring. Both solutions are then mixed together. The mixture was heated at 80 °C under continuous stirring was further for half an hour. Citric acid was added into the mixture drop by drop till its pH value reached up to 1.5. After this the stirring was extended further for more half an hour and then ammonia solution was added to the mixture till the pH value reached up to 6. The heating and stirring were continued further for 20 minutes. After that the stirring was stopped but the heating was continued further till the formation of a transparent gel. This gel was aged for 24 hours at room temperature and then dried at 100 °C for two hours. Finally the crystals as obtained were grounded and all the as prepared samples were annealed at 600 °C in steps of 100 °C for 4 hours. These samples were labeled as 0.0% AZO, 0.5% AZO and .0% AZO.

The analysis of the crystalline properties such as phase, structure and grain size was investigated by powder X-ray diffractographs (Schimadzu LabX- 6100 at Garware College, Pune) with an incident wavelength of 1.54 Å. The surface morphology of the as-prepared samples was investigated using the scanning electron microscopy (SEM) using a JEOL, JSM 5600 microscope at the Physics Department, SPPU, Pune. The band-gap energies of all the samples were determined from the UV–vis-spectroscopy measurements carried out at the Central Facility at Garware College, Pune.

## 3. RESULTS AND DISCUSSIONS:

### 3.1: Structural Analysis:

One requires detailed knowledge of the crystal structure and distribution of cations over the interstitial sites to understand the physical properties of that material. Such detailed structural information including cation distribution over the interstitial sites can be obtained by diffraction technique. The X-ray analysis is widely used to determine the crystal structure and the phase of the nanoparticles. The X-ray diffractograph is conducted in the range 10 – 80 degrees as shown in the Figure 1.

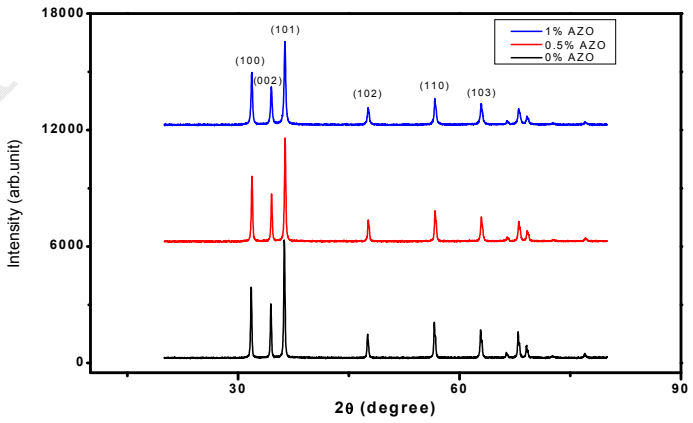


**Figure 1: X-Ray Diffractographs for the Undoped and Al doped ZnO Nanoparticles**

Figure 1 shows comparative X-ray diffraction patterns of x wt. % AZO samples with x = 0.0, 0.5 and 1.0 calcined at 600 °C. The finite width of the diffraction peaks confirms the formation of nanoparticles. The diffraction peaks corresponding to the diffraction planes (100), (002), (101), (102), (110) and (103) are observed in the diffraction patterns. These diffraction peaks match well and indexed to the JCPDS data sheet 050664 indicating the formation of Wurtzite structure of the ZnO nanoparticles. Since the XRD patterns of all the samples with different Al doped ZnO compositions retain the same structure of undoped ZnO, it indicates that Al doping has not changed the crystal structure of zinc oxide. Moreover, absence of any extraneous peak confirms the purity of the sample. The average crystalline size D of the as prepared nanoparticles is calculated by using Debye Scherrer's equation [25]

$$D = \frac{0.9\lambda}{(\beta Cos\theta)}$$

where $\lambda$ = wavelength of the incident light = 0.154 nm

$\beta$ = full width at half maxima (FWHM) of a diffraction peak

$\theta$ = Bragg's diffraction angle.

The particle size calculated from the XRD is 81 nm for undoped ZnO which decreases up to 61 nm for 1.0% Al doped ZnO. As seen from the XRD, increase in Al doping has increased the width of the diffraction peaks and the d spacing. This is due to the different sizes of the $Al^{+3}$ ion and $Zn^{+2}$ ion. Al has smaller ionic radius (0.054 nm) as compared to the Zn (0.074 nm). Hence when Al is doped into the ZnO structure, Al ions are substituted in the lattice by replacing Zn ions and without changing the structure of the undoped ZnO.

The various parameters such as FWHM, particle size and the d spacing evaluated from the XRD are tabulated in the Table 1 given below.

**Table1: Parameters such as FWHM, particle size and d spacing evaluated from the XRD**

| Sample | FWHM β (Rad) | d spacing (Å) | Particle Size D (nm) |
|---|---|---|---|
| 0.0% AZO | 0.0018 | 2.475 | 80.45 |
| 0.5% AZO | 0.0020 | 2.468 | 72.23 |
| 1.0% AZO | 0.0024 | 2.470 | 61.25 |

### 3.2: SEM Analysis

The morphological evolution of undoped and Al doped ZnO samples are carried out by scanning electron microscopy. The SEM images of the undoped and 1.0% Al doped ZnO samples are shown in the Figure 2 (a-b). Well dispersed, uniform spherical particles of undoped and 1.0% Al doped ZnO samples are observed.

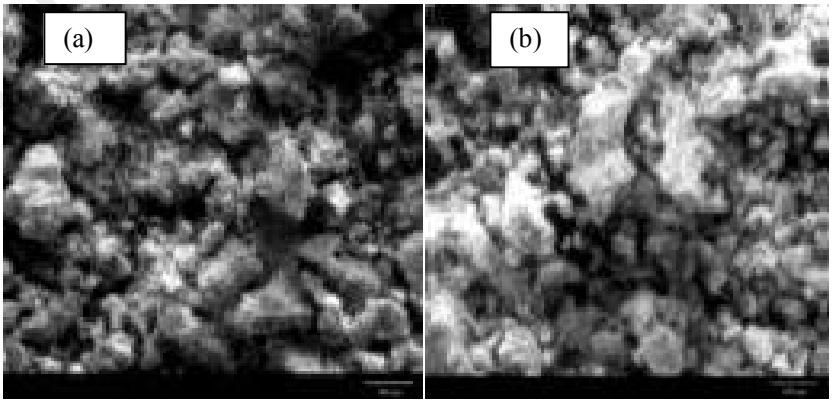


**Figure 2(a-b): SEM images of undoped and 1.0% Al doped ZnO**

### 3.3: Optical Measurements

In deciding the performance of a device, optical properties of any material plays a very important role. Using the UV-visible spectrophotometer, the absorption spectra are recorded at room temperature for the as prepared undoped and doped AZO nanoparticles within the wavelength range 300-500 nm and are shown in the Fig.3 (a)-(c).

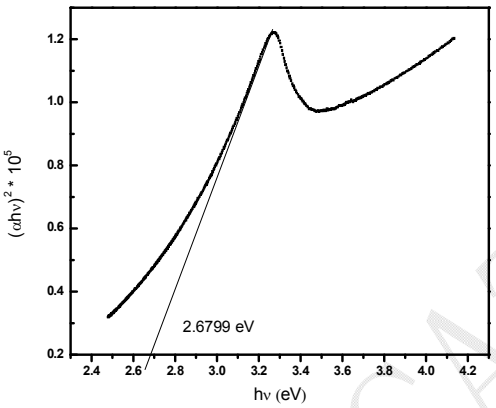


**Figure 3 (a): Tauc Plot for Undoped AZO**

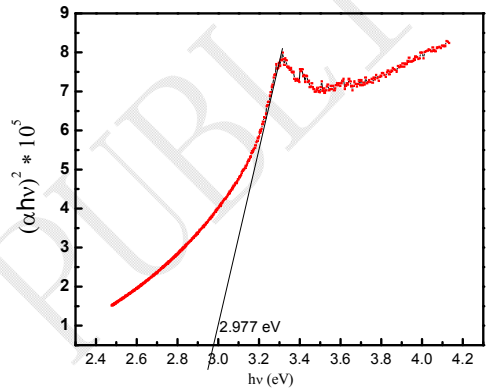


**Figure 3 (b): Tauc Plot for 0.5% doped AZO**

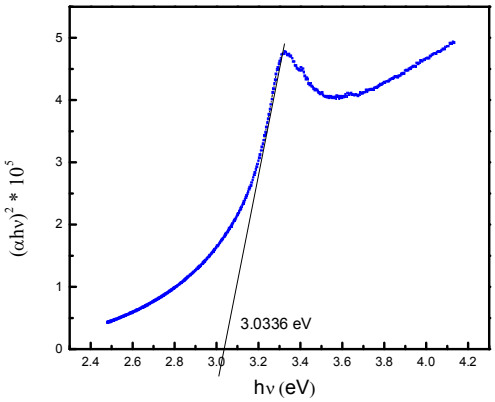


**Figure 3 (c): Tauc Plot for 1.0% doped AZO**

The Tauc equation [26] is exploited to determine the optical band gap

$$\alpha h\nu = c(h\nu - E_g)^{\frac{1}{2}}$$

Where hν = the photon energy

$E_g$ = the band gap energy and

c = a constant.

A Tauc plot is plotted for each sample by taking $(\alpha h\nu)^2$ along Y-axis and hν along X-axis. After extrapolating the linear portion of the plot of $(\alpha h\nu)^2$ vs hν to the energy axis, the value of the energy band gap can be achieved. From the optical properties it is observed that as the doping increases, the absorption wavelength shifts towards lower values and the band gap energy also increases from 2.68 eV to 3.03 eV for undoped and 1.0% doped AZO respectively. These results are tabulated in the Table 2.

**Table 2: Results of UV-vis Absorption Spectroscopy**

| Sample | Absorption wavelength (nm) | Band gap energy (eV) |
|---|---|---|
| Undoped AZO | **378** | **2.68** |
| 0.5% doped AZO | **375** | **2.98** |
| 1.0% doped AZO | **373** | **3.03** |

## 4.CONCLUSIONS:

Undoped and aluminium doped zinc oxide nanoparticles are successfully synthesized by sol-gel method. The doping of aluminium is successfully conducted for 0.5% and 1.0% samples. The particle size is found to decrease from 80 nm to 61 nm as the doping percentage increase. The bang gap energy also increases along with the doping there by making the material suitable for optical devices.

## REFERENCES:

1) Liu ZW, Lee H, Xiong Y, Sun C, Zhang X (2007) Far-field optical hyperlens magnifying sub-diffraction-limited objects. Science 315(5819):1686–1686.
2) Cai WS, Chettiar UK, Kildishev AV, Shalaev VM (2007) Optical cloaking with metamaterials. Nat Photonics 1(4):224–227.
3) Soukoulis CM, Linden S, Wegener M (2007) Negative refractive index at optical wavelengths. Science 315(5808):47–49.
4) Wang Z, Zhang R, Guo J (2018) Quadrupole mode plasmon resonance enabled subwavelength metal-dielectric grating optical reflection filters. Opt Express 26(1):496–504

5) Lin JY, Zhong KD, Lee PT (2016) Plasmonic behaviors of metallic AZO thin film and AZO nanodisk array. Opt Express 24(5):5125–5135
6) Naik GV, Schroeder JL, Ni X, Kildishev AV, Sands TD, Boltasseva A (2012) Titanium nitride as a plasmonic material for visible and near-infrared wavelengths. Opt Mater Express 2(4):478–489
7) J. Bao, M. A. Zimmler, F. Capasso, X. Wang and Z. F. Ren, Nano Lett. **6**, 1719 (2006).
8) H. C. Cheng, C. F. Chen and C. Y. Tsay, Appl. Phys. Lett. **90**, 012113 (2007).
9) P. P. Sahay and R. K. Nath, Sens. Actuators B **133**, 222 (2008).
10) J. Xu, C. Yuping, L. Yadong and S. Jianian, J. Mater. Sci. **40**, 2919 (2005).
11) R. Ramasubramaniam, J. Chen, H.Y. Liu, Homogeneous carbon nanotube/polymer composites for electrical applications. Appl. Phys. Lett. 83, 2928-2930 (2003).
12) S. H. Lee, S.H. Jeon, J.R. Youn et al., Rheological and electrical properties of polypropylene composites containing functionalized multi-walled carbon nanotubes and compatibilizers. Carbon 45, 2810–2822 (2007).
13) S. Benramache, O. Belahssen, H. Ben Temam, *Int. J. Renewable Energ. Res.* **4**, 1009 (2014).
14) S. Benramache, B. Benhaoua, O. Belahssen, *Optik* **125**, 5864 (2014).
15) H. Serier, M. Gaudon and M. Menetrier, *Solid State Sci.* **11**, 1192 (2009).
16) A. Verma, F. Khan, D. Kar, B. C. Chakravarty, S. N. Singh and M. Husain, *Thin Solid Films* **518**, 2649 (2010).
17) T. Ogi, D. Hidayat, F. Iskandar, A. Purwanto and K. Okuyama, *Adv Powder Technol*. **20, 203 (2009).**
18) Gonzáles A E Jimenes 1998 *Journal of Crystal Growth* **192** p. 430-438.
19) S. K. Pandian, K. Karthik, K. Sureshkumar et al., Effect of Mn doping on structural, optical, and Dielectric properties of $SnO_2$ nanoparticles by coprecipitation method. Mater. Manuf. Processes 27, 130–134 (2012).
20) O. Lupan, L. Chow, L.K. Ono et al., Synthesis and characterization of Ag-or Sb-doped ZnO nanorods by a facile hydrothermal route. J. Phys. Chem. 114, 12401–12408 (2010).
21) B. J. Jin, S. Im, S.Y. Lee, Violet and UV luminescence emitted from ZnO thin films grown on sapphire by pulsed laser deposition. Thin Solid Films 366, 107–110 (2000).
22) M. S. Aida, N. Bouhssira, S. Abed et al., Influence of annealing temperature on the properties of ZnO thin films deposited by thermal evaporation. Appl. Surf. Sci. 252, 5594–5597 (2006).
23) H. B. Zhou, H.Y. Zhang, M.L. Tan et al., Effects of substrate temperature on the efficiency of hydrogen incorporation on the properties of Al-doped ZnO films. Superlattices Microstruct. 51, 644–650 (2012).
24) Y. C. Kong, D.P. Yu, B. Zhang et al., Ultraviolet-emitting ZnO nanowires synthesized by a physical vapor deposition approach. Appl. Phys. Lett. 78, 407–409 (2001).
25) H. P. Klug, L.E. Alexander, X-ray Diffraction Procedures for Polycrystalline and Amorphous Materials, John Wiley, 1974.
26) J. Tauc. Amorphous and Liquid Semiconductors, Plenum, 1974.